ACADEMIA | Letters

Butterworth pattern-based selective zero placement of a combined damping and tracking controller for high-bandwidth nanopositioning

Mohammed Altaher PhD-MSc-BSc-MIET
mohammed.t.altaher@outlook.com
Rahul Jagdish Moon, Teesside University
r.moon@tees.ac.uk
February 14, 2022

Reference tracking control of periodic ramp-like signals is a requirement in nanopositioning applications. Such applications involve atomic force microscopes [1], high density data storage devices [2], lab-on-a-chip devices [3], nanolithography [4], optical systems [5] and nanomachining [6] and so on. These signals are high-frequency components and therefore any control system should exhibit a maximum flat-band low pass filter characteristic in order to accurately track such signals. The Butterworth filter is known to have a maximum flat-band frequency response and any control system emulating its behaviour should track ramp-like signals accurately. Further, vibration and nonlinearities such as hysteresis are primary problems associated with a piezo-driven nanopositioner. The damping loop uses the Integral Resonant Controller (IRC) to deal with vibration, and the tracking loop uses the Integral (I) or Proportional Integral (PI) to deal with uncertainties. The IRC introduces a low-frequency pole into the tracking-loop affecting the bandwidth of the closed-loop. This letter presents a PI feedback control with a selective zero placement imitating the Butterworth filter frequency response and negating the IRC pole without significant contribution to phase shift profile of the system. The designed control strategy offers 34% improvement in bandwidth, and the performance is tested using experimental validation. This improvement in the bandwidth is of vital importance to capturing the major harmonics of the ramp-like signals, such as a triangular wave.

Academia Letters, February 2022

Corresponding Author: Mohammed Altaher, mohammed.t.altaher@outlook.com
Citation: TK.

The common control closed-loop approach is to invoke two loops for better performance of the nanopositioners. The two loops, damping and tracking loop, are applied simultaneously. The damping loop is associated with employing a damping controller in the system to damp the mechanical resonant of the nanopositioner and facilitate a high-gain tracking controller in the tracking loop. There are various types of damping controllers used in the literature, such as Integral Resonant Control (IRC) [7]. The tracking loop is associated with the reduction of errors from uncertainties such as hysteresis and creep. There are various types of tracking controllers employed, such as an Integral (I) [8], or a Proportional-Integral (PI) [9], controllers. The IRC, a simple and robust damping controller, will be used in this letter. However, the IRC introduces a low-frequency pole, thereby limiting the bandwidth. Simultaneous design improvements for damping and tracking controllers are reported in [10]. However, this control scheme does not deliver a substantially superior positioning performance over a wider bandwidth. This is because such methods employ a first-order integrator to track a triangular trajectory without cancelling the pole of the IRC, which limits the bandwidth and increases the phase profile of the closed-loop damped system. The reason for selecting PI rather than I controller is due to the IRC's low-frequency pole. The PI controller negates the IRC pole, which increases the bandwidth. Recent research introduces the PI controller as a tracking controller in the context of nanopositioning, as reported in [11]. On the other hand, cancelling the IRC pole entirely is not beneficial and has a limited bandwidth. A further method using a PI controller is reported in [12]; however, the design method of the controller parameters is not systematic. Another traditional method is reported in [13] using mimicry of the Butterworth. However, this method is based on a single integral action which do not cancel the IRC pole.

This letter proposes the IRC in the damping loop integrated with a PI controller in the tracking loop. The closed-loop bandwidth of the proposed controller mimics the Butterworth frequency response and the zero of the proposed PI is selected to achieve the best bandwidth. Consider the feedback schemes depicted in Figure 1. The input reference is referred to as r,

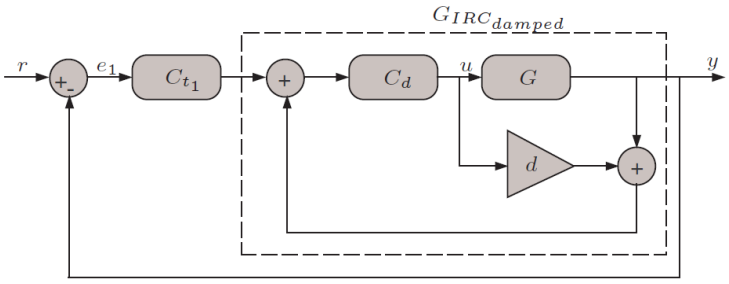

Figure 1. Block diagrams for the traditional control scheme.

Corresponding Author: Mohammed Altaher, mohammed.t.altaher@outlook.com
Citation: TK.

y is the output, G is the plant, C_d is the damping gain, C_t is the tracking gain, and d is the feed-through term. The G(s) is given by:

$$G(s) = \frac{\sigma^2}{s^2 + 2\zeta\omega_p s + \omega_p^2}, \tag{1}$$

where ζ is the damping ratio, ω_p is the natural frequency and σ^2 is chosen to adjust the gain of the stage at 0 Hz frequency. The proposed control strategy uses a systematic approach in identifying the PI controller parameters, engaging the Butterworth filter pattern to achieve the maximum bandwidth of the closed-loop. The tracking controller is given by:

$$C_{t_1} = \frac{K_i(s + \omega_z)}{s\omega_z} \tag{2}$$

The closed-loop transfer function with respect to Figure 1 is given by:

$$s^4 + (2\zeta\omega_p - dK_d)s^3 + (\omega_p^2 - 2\zeta dk_d\omega_p)s^2 + (\frac{\sigma^2 K_d K_i}{w_z} - \sigma^2 K_d - dK_d\omega_p^2)s + \sigma^2 K_d K_i = 0 \tag{3}$$

The characteristics equation of the fourth-order Butterworth filter at any given frequency (ω_c) is given by:

$$s^4 + 2.6132\omega_c s^3 + 3.4143\omega_c^2 s^2 + 2.6132\omega_c^3 s + \omega_c^4 \tag{4}$$

In order to emulate the Butterworth pattern, the characteristics equation for the proposed PI controller must be equated with the characteristics equation for the Butterworth filter; this will determine the values for the feed-through term, damping gain and tracking gain. Thus, (3) must be similar to (4). The following quantities are obtained as a result of linking the two characteristics equations:

$$\left\{ \begin{array}{c} 2.6132\omega_c = 2\zeta\omega_p - dK_d \\ 3.414\omega_c^2 = \omega_p^2 - 2\zeta\omega_p dK_d \\ 2.6132\omega_c^3 = K_d[\frac{\sigma^2 K_i}{\omega_z} - \sigma^2 - d\omega_p^2] \\ \omega_c^4 = \sigma^2 K_d K_i \end{array} \right\} \tag{5}$$

Corresponding Author: Mohammed Altaher, mohammed.t.altaher@outlook.com
Citation: TK.

As a result of equating the above equations, the following is obtained:

$$\omega_c^2 - 1.5307\zeta\omega_p\omega_c + \frac{\omega_p^2(4\zeta^2 - 1)}{3.4143} \tag{6}$$

the above equation can be solved as below:

$$\omega_c = \frac{5.2264\zeta\omega_p \pm \sqrt{27.3153\zeta^2\omega_p^2 - 13.6572(4\zeta^2\omega_p^2 - \omega_p^2)}}{6.8286} \tag{7}$$

The values of ω_p and ζ are known from the system in equation 1, therefore ω_c can be calculated (positive value is considered). In the same manner, the value of the damping gain can be evaluated using the following formula:

$$K_d = \frac{2.6132(\omega_c^3\omega_z 2\zeta) - 2\omega_c^4\zeta + \omega_c^3\omega_z - 3.4143(\omega_c^2\omega_p\omega_z)}{-2\zeta\sigma^2\omega_z} \tag{8}$$

As can be seen from the above equation, that the value of damping gain is reliant on the zero of the PI (ω_z). The system has complex conjugate pair poles, plus a pole on the x-axis (real pole introduced by the IRC). In total four poles are required to form the Butterworth fourth-order. The proposed PI controller has a real pole at zero frequency and a zero at ω_z frequency, in addition to two poles of the system. The value of the feed-through term d can be determined using the following formula:

$$d = \frac{2\zeta\omega_p - 2.6132\omega_c}{K_d} \tag{9}$$

The value of the tracking gain of the PI controller can be calculated as in the following equation:

$$K_i = \frac{\omega_c^4}{K_d\sigma^2} \tag{10}$$

In order to find the optimal value of ω_z for the proposed controller, Figure 2(a and b) depicts the optimal values for ω_z such that the bandwidth of the closed-loop of the proposed PI-Butterworth must not deviate from the 0 dB line by $\pm$ 1 dB or $\pm$3 dB.

Corresponding Author: Mohammed Altaher, mohammed.t.altaher@outlook.com
Citation: TK.

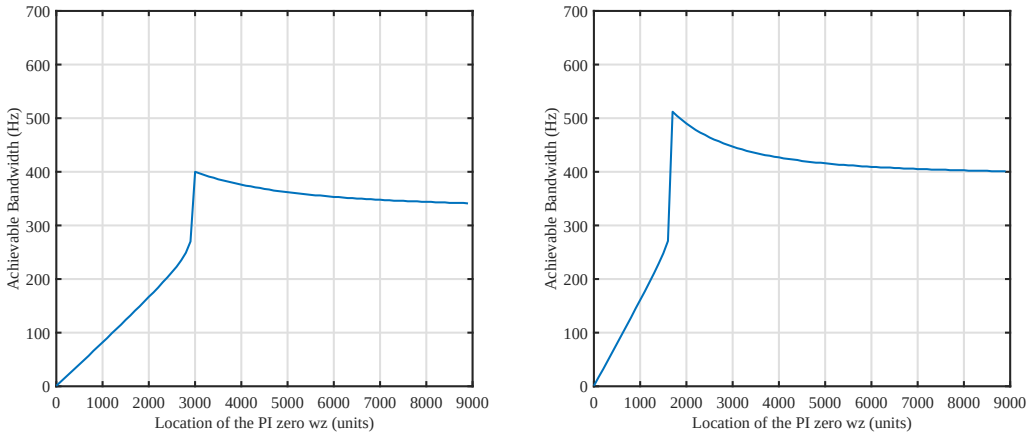

Figure 2. The optimal value of ω_z for the proposed PI-Butterworth: (a) deviation from 0 dB is less than $\pm$1 dB; and (b) deviation from 0 dB is less than $\pm$3 dB.

Two values of ω_z are selected based on $\pm$ 1 or 3 dB from 0 dB, achieving maximum bandwidth so that ω_z is not the same frequency as the pole introduced by the IRC. The following table provides the values of the controller parameters of the proposed system so the closed-loop bandwidth mimics the Butterworth frequency response.

Table 1. Tabulates the proposed controller parameters

± 1 **from 0** dB				
K_d	K_i	d	ω_c	ω_z
10268	366.2722	-0.6199	2470.9 $\frac{rad}{sec}$	3000 $\frac{rad}{sec}$
± 3 **from 0** dB				
K_d	K_i	d	ω_c	ω_z
11227	334.9958	-0.5669	2470.9 $\frac{rad}{sec}$	1700 $\frac{rad}{sec}$

It is important to note that the value of ω_c is independent of the zero introduced by the PI and therefore it remains unchanged for any given value of the ω_z. The mimicry of the Butterworth filter through PI than I as in [13] has the advantage of reducing the phase of the system and manipulating the system properties through the choice of ω_z. It also simplifies the relationship between the damping and tracking controllers. The pole-zero map of the traditional and proposed methods is plotted in Figure 3(a and b). It can be seen that the pole of the IRC at ω_c=4066.8 $\frac{rad}{sec}$ is cancelled using the zero of the PI with the traditional method.

Corresponding Author: Mohammed Altaher, mohammed.t.altaher@outlook.com
Citation: TK.

However, the closed-loop system poles are closed to the imaginary axis, thereby affecting the stability of the system. As the traditional I-Butterworth and PI-Butterworth exhibit the same ω_c, it can be seen the four poles of the Butterworth are almost identical and equally distributed to form the Butterworth pattern, although there is a slight difference in the location of the poles. However, the critical advantages of the proposed method lie in negating the IRC police via the zero of the proposed PI-Butterworth using selective placement, as in Figure 3(a) ω_z is 3000 $\frac{rad}{sec}$ and in Figure 3(b) ω_z is 1700 $\frac{rad}{sec}$.

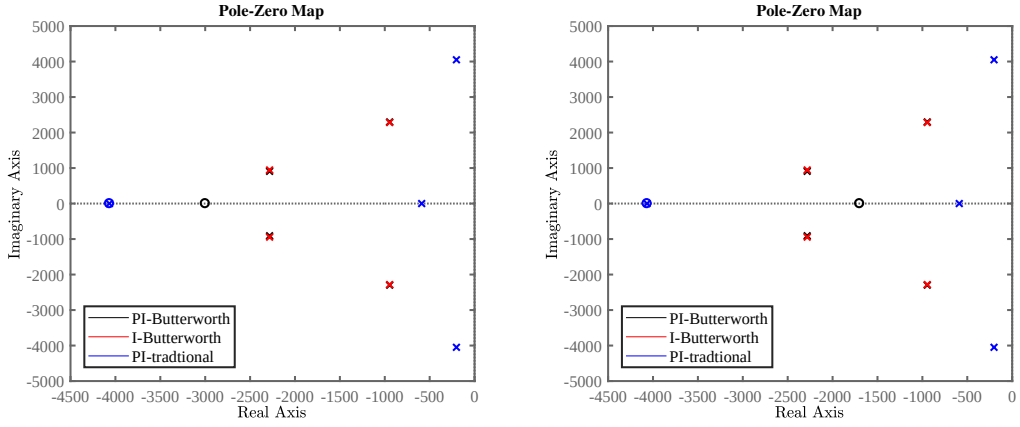

(a) (b)

Figure 3. Comparison of the pole-zero map of the Butterworth-based-I and -PI versus traditional PI (a) ω_z for the PI-Butterworth-based is 3000 $\frac{rad}{sec}$; and (b) ω_z for the PI-Butterworth-based is 1700 $\frac{rad}{sec}$.

The design procedures for the proposed control method guarantee stability and offer maximum flat passband. This exhibits high stability margins and therefore it is robust to uncertainties and disturbances. The stability margin for the proposed control system gain margin (GM) is around 9 dB. The phase margin (PM) is around 55°. In practice the stability is tested and the system is stable. A triangular wave is traced reasonably well by a closed-loop control system whose bandwidth is sufficient to capture the major harmonics that form the triangular wave. The higher the bandwidth, the better the trace for triangular wave. The following figures provide a comparison of the closed-loop bandwidth using the traditional and proposed methods where the dotted black line is $\pm$3 dB. The selected value of ω_z is 3000 $\frac{rad}{sec}$ for the proposed PI-Butterworth and deviation from 0 dB is less than $\pm$1 dB. Although recent research proposes that 3dB deviation is acceptable [14], this can increase the proposed method's bandwidth.

Corresponding Author: Mohammed Altaher, mohammed.t.altaher@outlook.com
Citation: TK.

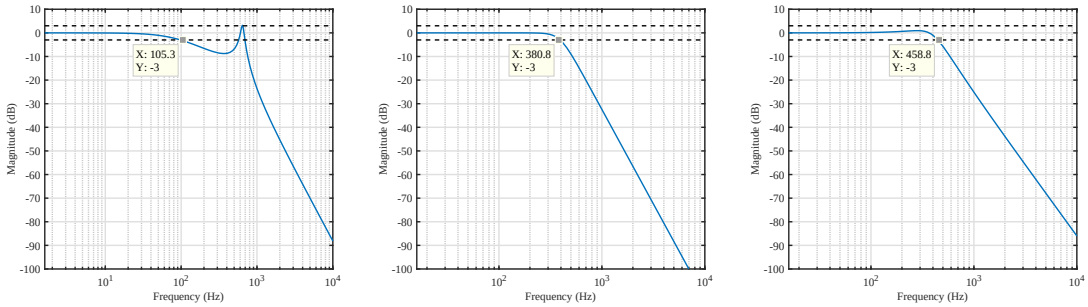

(a) (b) (c)

Figure 4. (a) Closed-loop bandwidth for the traditional control scheme using PI; and (b) closed-loop bandwidth for the traditional control scheme using I; and (c) closed-loop bandwidth for the proposed control scheme using PI.

Table 2 presents the achievable bandwidth for the closed-loop for both traditional and proposed methods.

Table 2. Tabulates the obtained bandwidth

PI-traditional	**I-Butterworth**	**PI-Butterworth**
105.3 Hz	380.8 Hz	458.8 Hz

The control system design based on frequency response shows the proposed controller is practically implementable.

The PI-Butterworth shows moderate phase distortion. Thus, the calculated phase-response of the proposed PI agrees with the expected phase response due to pole-zero cancellation. The improved Butterworth using PI has achieved a low-pass filter characteristic with maximally flat amplitude within the filter passband. Magnitude response is almost flat for a significant duration of the closed-loop bandwidth, for which satisfactory set-point tracking occurs. The Closed-loop Frequency Response Data (FRD) for the proposed PI-Butterworth is plotted in Figure 5. The advantage of FRD analysis for controller design is ensuring the desired closed-loop characteristics are practically implementable. The FRD analysis or bode plot also includes information about stability with time delays. The PI-Butterworth shows moderate phase distortion. Thus, the calculated phase-response of the proposed PI agrees with the expected phase response due to pole-zero cancellation. The improved Butterworth using PI has achieved a low-pass filter characteristic with maximally flat amplitude within the filter

Corresponding Author: Mohammed Altaher, mohammed.t.altaher@outlook.com
Citation: TK.

passband. The system is experimentally stable from the observed GM and PM. Magnitude response is almost flat for a significant duration of the closed-loop bandwidth, for which satisfactory set-point tracking occurs. It can be concluded that control system design based on frequency response analysis is satisfactory.

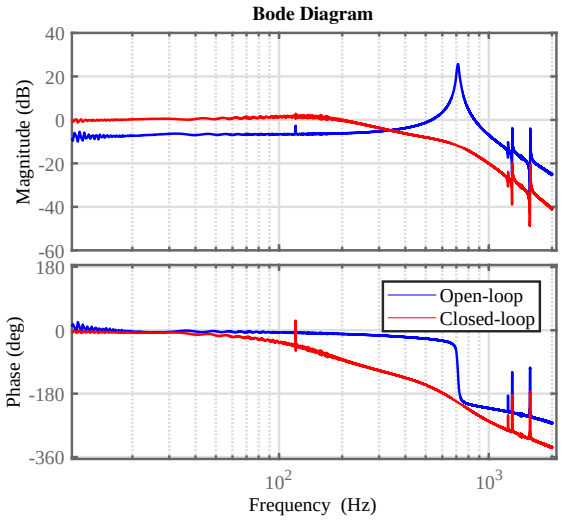

Figure 5. The Closed-loop Frequency Response Data (FRD) for the proposed PI-Butterworth.

For the realisation and evaluation of the proposed method by means of performance in time-domain in the presence of disturbances such as hysteresis, Figure 6(a) presents time domain reference tracking for 5 Hz triangular trajectory. Figure 6(b) shows root mean square position error (RMSE) for triangular references over a range of frequencies to justify the improvement in bandwidth in comparison to the traditional method I-Butterworth.

Corresponding Author: Mohammed Altaher, mohammed.t.altaher@outlook.com
Citation: TK.

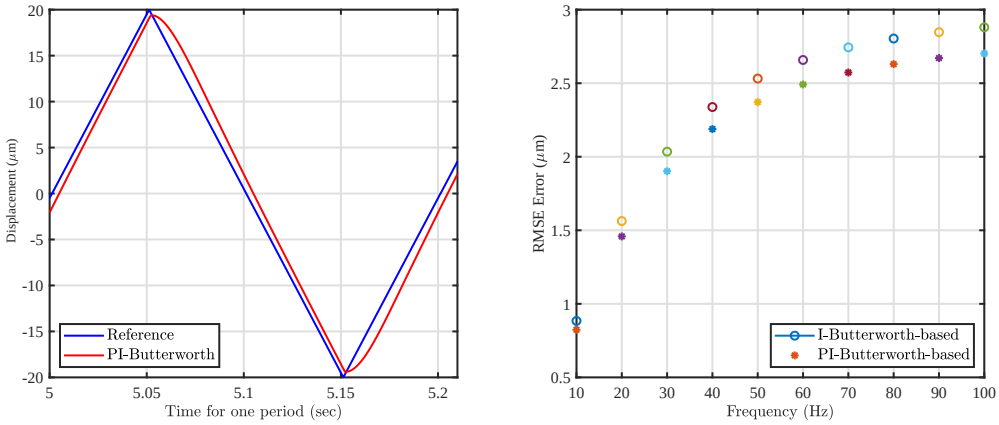

(a) (b)

Figure 6. (a) The time-domain tracking performance for PI-Butterworth in the presence of disturbances; and (b) comparison of the RMSE for triangular trajectories with different fundamental frequencies.

As expected, in line with the obtained increased bandwidth, the proposed method produces less error in comparison to the traditional method. This piece of work effectively increases the positioning bandwidth of the nanopositioner by about 34% via selective zero placement. The controller parameters are derived analytically. Simulation and experimental results are in close agreement and validate the proposed control scheme. Future work will involve parameter optimisation.

Corresponding Author: Mohammed Altaher, mohammed.t.altaher@outlook.com
Citation: TK.

References

[1] Chung-Feng Jeffrey Kuo, Vu Quang Huy, Chin-Hsun Chiu, and Shou-Feng Chiu. Dynamic modeling and control of an atomic force microscope probe measurement system. *Journal of Vibration and Control*, 18(1):101–116, 2012.

[2] Abu Sebastian, Angeliki Pantazi, Haris Pozidis, and Evangelos Eleftheriou. Nanopositioning for probe-based data storage [applications of control]. *IEEE Control Systems*, 28(4), 2008.

[3] Anandakumar Sarella, Andrea Torti, Marco Donolato, Matteo Pancaldi, and Paolo Vavassori. Two-dimensional programmable manipulation of magnetic nanoparticles on-chip. *Advanced Materials*, 26(15):2384–2390, 2014.

[4] Ping Gao, Xiong Li, Zeyu Zhao, Xiaoliang Ma, Mingbo Pu, Changtao Wang, and Xiangang Luo. Pushing the plasmonic imaging nanolithography to nano-manufacturing. *Optics Communications*, 2017.

[5] ChaBum Lee. *Long-Range Nano-Scanning Devices Based on Optical Sensing Technology*, pages 495–522. Advanced Mechatronics and MEMS Devices II. Springer, 2017.

[6] Zhiwei Zhu, Suet To, Kornel F. Ehmann, and Xiaoqin Zhou. Design, analysis, and realization of a novel piezoelectrically actuated rotary spatial vibration system for micro-/nano-machining. *IEEE/ASME Transactions on Mechatronics*, 2017.

[7] Yik R. Teo, Douglas Russell, Sumeet S. Aphale, and Andrew J. Fleming. Optimal integral force feedback and structured pi tracking control: Application for objective lens positioner. *Mechatronics*, 24(6):701–711, 2014.

[8] Ryan R. Orszulik and Jinjun Shan. Output feedback integral control of piezoelectric actuators considering hysteresis. *Precision Engineering*, 47:90–96, 1 2017.

[9] C. X. Li, Y. Ding, G. Y. Gu, and L. M. Zhu. Damping control of piezo-actuated nanopositioning stages with recursive delayed position feedback. *IEEE/ASME Transactions on Mechatronics*, 22(2):855–864, 2017. ID: 1.

[10] Mohammad Namavar, Andrew J. Fleming, Majid Aleyaasin, K. Nakkeeran, and Sumeet S. Aphale. An analytical approach to integral resonant control of second-order systems. *IEEE/ASME Transactions on Mechatronics*, 19(2):651–659, 2014.

Corresponding Author: Mohammed Altaher, mohammed.t.altaher@outlook.com
Citation: TK.

[11] Andrew J. Fleming, Yik Ren Teo, and Kam K. Leang. Low-order damping and tracking control for scanning probe systems. *Frontiers in Mechanical Engineering*, 1:14, 2015.

[12] Mohammed Altaher and Sumeet S. Aphale. Enhanced positioning bandwidth in nanopositioners via strategic pole placement of the tracking controller. *Vibration*, 2(1):49–63, 2019.

[13] Douglas Russell, Andres San-Millan, Vicente Feliu, and Sumeet S. Aphale. Butterworth pattern-based simultaneous damping and tracking controller designs for nanopositioning systems. *Frontiers in Mechanical Engineering*, 2:2, 2016.

[14] Linlin LI, Sumeet S. Aphale, and Limin ZHU. High-bandwidth nanopositioning via active control of system resonance. *Front. Mech. Eng*, 2(16):331–339, 2021.

Corresponding Author: Mohammed Altaher, mohammed.t.altaher@outlook.com
Citation: TK.